

Tổng hợp xanh vật liệu khung kim loại-hữu cơ Cu₃BTC₂ loại bỏ methylene blue trong môi trường nước

TÓM TẮT

Nghiên cứu này trình bày kết quả nghiên cứu tổng hợp, mô tả đặc trưng và khả năng hấp phụ của vật liệu khung cơ kim trên cơ sở Cu(II) và phổi tử hữu cơ 1,3,5-benzene tricarboxylate (Cu-BTC). Cu-BTC được tổng hợp bằng phương pháp vi sóng đơn giản và được đo FTIR, SEM, XRD để kiểm tra đặc tính liên kết, hình thái, cấu trúc tinh thể. Cu-BTC được sử dụng làm chất hấp phụ để loại bỏ thuốc nhuộm họ azo như methylene blue (MB) trong nước. Các nghiên cứu về ảnh hưởng của pH, nồng độ, thời gian hấp phụ cho thấy loại bỏ MB theo mô hình hấp phụ đẳng nhiệt Freundlich và mô hình động học biểu kiến bậc hai. Do đó, cơ chế hấp phụ MB đa lớp trên bề mặt Cu-BTC không đồng nhất và chịu ảnh hưởng của lực hút tĩnh điện. Những đặc trưng này cho thấy Cu-BTC là vật liệu hứa hẹn trong việc loại bỏ MB ra khỏi nước thải định hướng ứng dụng tiềm năng trong xử lý môi trường.

Keywords: Hóa học xanh, vật liệu khung kim loại-hữu cơ, kỹ thuật vi sóng, methylene blue, xử lý môi trường.

Green synthesis of metal-organic framework material Cu₃BTC₂ removes methylene blue from aqueous media

ABSTRACT

This study presents the results of the synthesis, characterization, and adsorption capacity of organometallic framework materials based on Cu(II) and the organic ligand 1,3,5-benzene tricarboxylate (Cu-BTC). Cu-BTC was synthesized by simple microwave method, and FTIR, SEM, and XRD were measured to check the bonding, morphology, and crystal structure properties. Cu-BTC is an adsorbent to remove azo dyes such as methylene blue (MB) from water. Studies on the effects of pH, concentration, and adsorption time showed that MB was removed according to the Freundlich isotherm adsorption model and the apparent second-order kinetic model. Therefore, the multilayer MB adsorption mechanism on the Cu-BTC surface is heterogeneous and influenced by electrostatic attraction. These characteristics show that Cu-BTC is a promising material for removing MB from wastewater with potential applications in environmental treatment.

Từ khóa: *Green chemistry, metal-organic frameworks, microwave method, methylene blue, environment treatment.*

1. INTRODUCTION

Textile industry wastewater has severe impacts on living organisms. It must be treated to a certain extent before being released into the environment. Dyeing process wastewater contains non-biodegradable and high-toxic pigments [1], which have been found to damage the balance [2-4] and integrity of ecological systems [5, 6] and have carcinogenic effects on long-term exposure [7-9]. Therefore, wastewater treatment in the textile dyeing industry has become a concern on a global scale [10, 11]. In this context, researchers have proposed metal-organic frameworks (MOFs) as one of the effective methods to remove dye wastewater [12-14]. Because MOF exhibits high adsorption capacity in dye removal with tunable pore diameter and surface morphology compared with other conventional adsorbent materials such as activated carbon [15, 16], carbon nanotubes [17], zeolite [18] ... In addition, the metal-organic framework material also has a significant photocatalytic activity for the treatment of different dye types [19-21]. These studies also evaluated the effectiveness of these MOFs in the process of dye removal from wastewater. Metal-organic frameworks based on copper (II) have also been synthesized, modified, combined, doped, hybridized... and evaluated for their ability to remove dyes in water environments [22, 23].

Many studies have applied different synthesis methods to fabricate copper-based metal-organic

frameworks. Solvothermal, one-step in situ growth and pre-grinding methods have all been studied to synthesize this material [24, 25]. Synthesis of MOFs has also been of interest to meet green chemistry requirements where selection of synthesis elements has been based on reduced energy input, safe reaction solvents (such as water and supercritical solvents), continuous manufacturing method, and performance design of MOFs through theoretical predictions [26, 27]. In this study, copper-based metal-organic framework (Cu-BTC) was synthesized green by microwave method using water/ethanol mixed solvent mixture. Cu-BTC was also evaluated for its ability to remove dyes in water by pure adsorption mechanism and simultaneous catalytic-adsorption mechanism.

2. EXPERIMENTAL

2.1. Chemicals, equipment and tools

Copper (II) chloride dihydrate (CuCl₂.2H₂O) (99%, Xilong Chemical Co., Ltd., Guangdong, China). 1,3,5-benzene tricarboxylic acid (H₃BTC) (98%, Shanghai Macklin Biochemical Co., Ltd., Shanghai, China). Ethanol solution (C₂H₅OH) (96%, Duc Giang Chemical, Vietnam). Methylene blue (C₁₆H₁₈ClN₃S, MB) (≥ 85%, Merck, Germany). Sodium hydroxide (NaOH) (> 96%, Duc Giang Chemical, Vietnam). Hydrochloric acid (HCl) (> 35%, Duc Giang Chemical, Vietnam). Double distilled water.

Electrolux microwave oven (50 Hz, 1050 W), China. Drying cabinet, China. Ultrasonic Cleaner Ultrasonic Cleaner JP-060S, China. Centrifuge Hettich Universal 320, Germany. Test tube shaker HY-4, Jiangsu, China. Shec qualitative filter paper, Shanghai, China. Laboratory glassware and some other common tools.

2.2. Material synthesis

The material was synthesized from CuCl_2 as follows: Weigh 1.7 g of $\text{CuCl}_2 \cdot 2\text{H}_2\text{O}$ into a 250 mL beaker, then add 100 mL distilled water, add 2.8 g H₃BTC acid, and stir well. Put the glass cup in the microwave (reaction conditions are 45 min, 80 °C). Next, filter and wash the precipitate with ethanol and distilled water 5 times using an ultrasonic cleaner, and then centrifuge at 7,000 rpm for 10 min with a centrifuge to obtain a very blue solid product. Then, the solid product is dried at 120 °C for 2 hours in a drying oven. Store the synthetic material in a tightly closed plastic container and use it for the following experiments.

2.3. Techniques and methods

Characterizations. Determination of the bonding characteristics of the metal-organic framework Cu-BTC by infrared spectroscopy method FTIR in the 400 to 4000 cm^{-1} wavelength range. SEM Hitachi S-4800 field emission scanning electron microscope (SEM) with magnification capability up to 100,000 times to measure the size and shape of nanostructured materials. The crystal structure of the Cu-BTC metallurgical framework material in powder form was analyzed through X-ray diffraction analyzer-D8-Advance. At 1.54 Å in a copper X-ray tube (Cu-K α), the device is operated at 44 mA and 40 kV voltage. The scanning speed is 0.2 °/min to measure materials in the range (2 θ) from 10 ° to 70 °.

Methylene blue adsorption. The MB solution (1 g/L) was diluted with distilled water twice to prepare the required MB solution concentrations (10, 20, 30, 40, and 50 mg/L). Methylene blue (MB) was used as a dye to study the adsorption capacity of the synthesized Cu-BTC organometallic framework. The pH of the MB solution was normalized with 1 M NaOH solution and 1 M HCl solution. Conducting experiments on the influence of pH on the MB adsorption process. 10 mg of Cu-BTC was added to each test tube containing 20 mL of MB solution. Each glass test tube with MB solution pH of 3, 5, 7, 9, and 11, respectively, was sealed with a rubber stopper, put into a closed light-blocking cabinet, and a light cabinet to study the effect of light. Then, the test tubes were

thoroughly mixed by ultrasonic washing for 15 min, shaken with a shaker at 200 rpm at room temperature to filter the solution, and finally photometrically. UV-Vis spectrum at maximum absorption wavelength to determine MB concentration based on the linear equation from the MB standard curve. Experiments to investigate the effect of pH on dye handling were carried out under the same conditions. Sample dilution was performed with double distilled water if the MB solution concentration value exceeded the maximum adsorption limit of the graph containing the MB calibration curve. Investigation of the kinetics of the adsorption process by influencing factors of pH, adsorption time, and initial MB solution concentration with the same amount of Cu-BTC adsorbent at equilibrium time was studied the same as above. The maximum wavelength of the MB solution is determined to be 662 nm. The equation can determine the concentration of MB solution at time t (unit is mg/L) to be

$$C = (\text{Abs} - 0.0216)/0.1587 \quad (R^2 = 0.9985),$$

where A is the light absorption intensity.

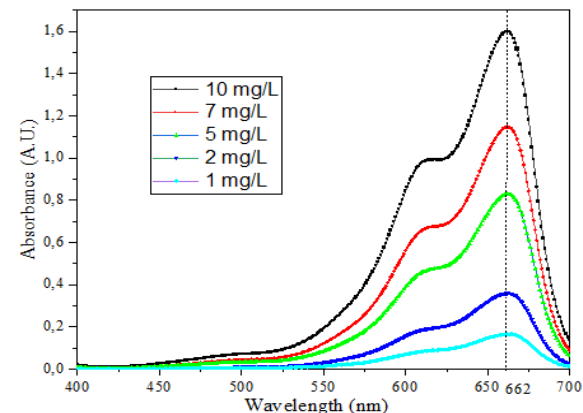


Figure 1. UV-Vis spectra of the MB standard sample at 400 to 700 nm wavelengths.

The MB removal efficiency of the material is calculated according to the equation:

$$H = \frac{C_0 - C_t}{C_0} \times 100\%$$

The adsorption capacity was calculated according to the formula:

$$q_t = \frac{V \times (C_0 - C_t)}{m}$$

Where C_0 and C_t are the initial concentration of MB solution and at time t (mg/L), respectively; V is the volume of MB solution used (L), and m is the mass of Cu-BTC (g).

Isothermal and kinetics of MB adsorption. Langmuir, Freundlich, and Temkin adsorption models are used to describe the adsorption equilibrium as follows:

$$\text{Langmuir model: } \frac{C_e}{q_e} = \frac{1}{K_L q_m} + \frac{C_e}{q_m}$$

$$\text{Freundlich model: } \ln q_e = \ln K_F + \frac{1}{n} \ln C_e$$

$$\text{Temkin model: } q_e = B_T \ln K_T + B_T \ln C_e$$

$$B_T = \frac{RT}{b_T}$$

In which q_e is the equilibrium adsorption capacity (mg/g), q_m is the maximum adsorption capacity (mg/g), K_L is the Langmuir constant (L/mg), K_F is the Freundlich [(mg/g)(L/mg) $^{1/n}$], and K_T is the Temkin constant (L/g); C_e is the equilibrium concentration of adsorbent (mg/L); n is Freundlich's linear constant, b_T is related to the adsorption heat, R is the universal gas constant and T is the temperature. The Langmuir adsorption model assumes that all adsorption sites have the same affinity and reach a maximum value for the adsorbent and adsorbate after forming a monolayer on a uniform adsorbent surface at a specific temperature and no interactions between the adsorbed molecules. In contrast to the Langmuir model, the Freundlich model assumes that the adsorption surface energy is heterogeneous. The n value represents the deviation from the linearity, the heterogeneity of the adsorption site. If n is between 1 and 10, then the adsorption is favorable. The larger n is, the higher the heterogeneity of the adsorption site. The Temkin is a chemical adsorption model based on the interaction between positive and negative charges.

To elucidate the adsorption kinetic process of MB on Cu-BTC, three apparent kinetic models, namely first-order, second-order, and intra-particle diffusion, are considered to explain the experimental data:

First-order apparent kinetic model:

$$\ln(q_e - q_t) = \ln(q_e) - k_1 t$$

Second-order apparent kinetic model:

$$\frac{t}{q_t} = \frac{1}{k_2 q_e^2} + \frac{t}{q_e}$$

$$\text{Particle diffusion model: } q_t = k_i t^{1/2} + C$$

In which q_e , q_t is the adsorption capacity at equilibrium time and at time t on the material (mg/g), respectively; k_1 is the first-order apparent adsorption rate constant (min^{-1}), k_2 is the second-order apparent adsorption rate constant ($\text{g}/(\text{mg} \cdot \text{min})$); C is the blocking coefficient in the particle and k_i is the diffusion rate constant in the particle ($\text{mg}/(\text{g} \cdot \text{min}^{1/2})$).

3. RESULTS AND DISCUSSION

3.1. Characterization

The FTIR spectra of the H_3BTC sample and the Cu-BTC organometallic framework material (Figure 2) contain characteristic peaks at ~ 1640 , ~ 1447 , and $\sim 1370 \text{ cm}^{-1}$. FTIR spectrum of Cu-BTC using KBr in the $400\text{-}1700 \text{ cm}^{-1}$ range. The peaks at ~ 1640 , ~ 1447 , and $\sim 1370 \text{ cm}^{-1}$ characteristically bond the carboxylate group -COO- in Cu-BTC, indicating the formation of Cu-BTC organometallic framework material [28, 29]. The broad bands at 3346 cm^{-1} are believed to be OH bonds and water adsorbed on the Cu-BTC surface. In addition, no peak was observed in the range of $1680\text{-}1750 \text{ cm}^{-1}$, which shows no free H_3BTC ligand in the Cu-BTC material [28]. The range $1500\text{-}1400 \text{ cm}^{-1}$ represents the C=C bond in the aromatic ring ⁴⁹. The FTIR shows the carbonyl group in H_3BTC peaks at 1721 cm^{-1} ⁵⁰. The -CO-C bond in Cu-BTC is demonstrated by the appearance of the peak at about 1109 cm^{-1} . The $827\text{-}1153 \text{ cm}^{-1}$ range belonged to the OC=O and CO bond of 1,4 benzene dicarboxylic acid. At 487 cm^{-1} and 728 cm^{-1} , it is assigned the CH bond of the benzene ring and the Cu-O bond form between the carboxylic groups of H_3BTC and Cu(II), respectively [30, 31].

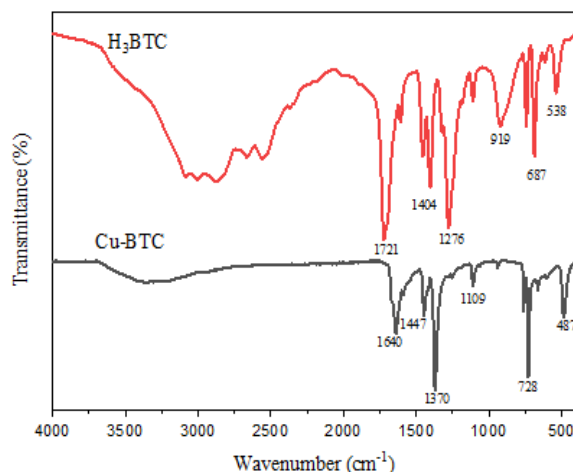


Figure 2. FTIR spectrum of H_3BTC and Cu-BTC.

SEM image of Cu-BTC material in Figure 3. Cu-BTC crystal particles have an octahedral shape. Cu-BTC morphology is consistent with other reported SEM images [28, 32, 33]. Some

particles that do not have a characteristic morphology in the SEM images are fused particles of Cu-BTC crystals.

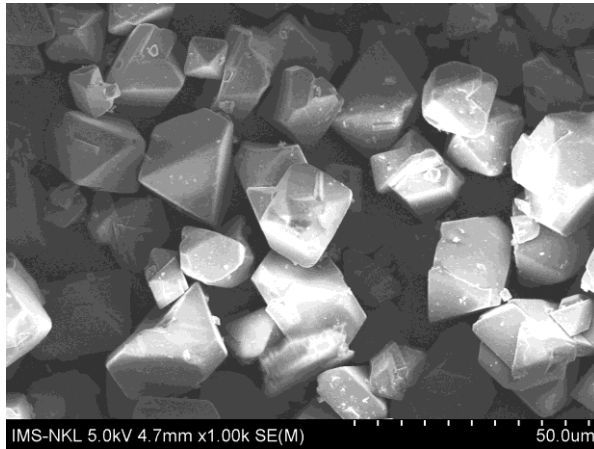


Figure 3. SEM images of Cu-BTC.

X-ray diffraction (XRD) analysis examined the crystal structure of the powdered Cu-BTC in Figure 4. The characteristic peaks are found in the Cu-BTC crystalline in the range up to 2θ , namely 11.6° , 13.5° , 14.9° , and 16.6° corresponding to the crystal faces (222), (400), (420), (422) and is consistent with the published study [28, 32, 34-37], which shows that metal-organic frameworks are successfully fabricated. The peak with the highest intensity at $2\theta = 11.59^\circ$ is related to the high degree of crystallinity of the material [30]. XRD and SEM spectrum results show the successful fabrication of Cu-BTC.

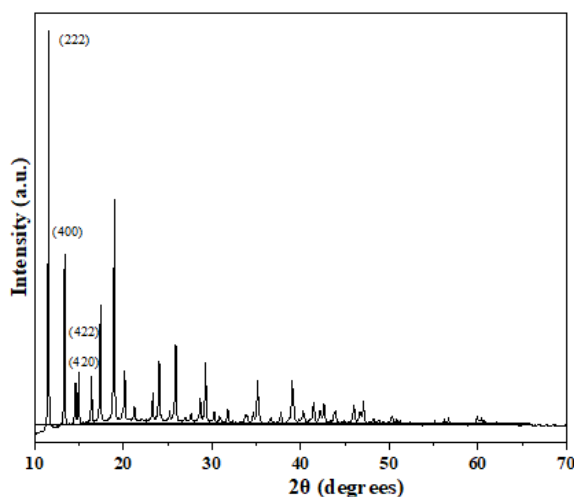


Figure 4. XRD patterns of Cu-BTC.

3.2. Effect of pH on the adsorption of methylene blue

The adsorption capacity of the MB solution is significantly influenced by its pH level [38]. Figure 5 and Table 1 show that the optimal pH for methylene blue adsorption onto Cu-BTC is

pH \sim 7. The results are similar to previous studies [30, 39].

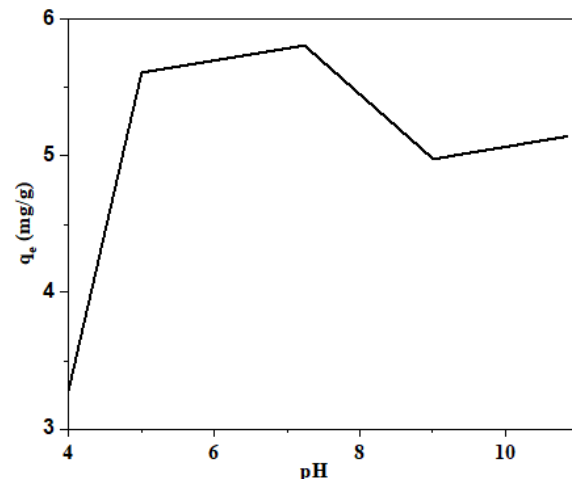


Figure 5. Effect of pH on the adsorption capacity of MB. Experimental conditions include 25°C , 0.011 g Cu-BTC.

The adsorption capacity of MB increases when the pH increases from 4 to 7. However, the adsorption capacity remained almost constant with an increase in pH from 7 to 11. The point of zero charge of pH (pHPZC) for Cu-BTC material was found to be 4.0 [40]. When $\text{pH} < 4$ the surface of the adsorbent turns positively charged, and the adsorption process of methylene blue onto Cu-BTC is difficult. When $\text{pH} \geq 4$, the surface of the adsorbent turns negatively charged, and this process is easy. When $4 \leq \text{pH} < 7$, H^+ ions compete with dye cations through electrostatic attraction causing a decrease in the amount of adsorption. It is possible that a low pH might not be suitable for adsorption of MB. When increasing pH, MB solution containing Cl^- binds to Cu-BTC material quickly and reacts with NaOH to form NaCl and MB-S+ OH . The mass of NaCl can change the adsorption of MB-S+ OH on the surface of Cu-BTC material. While $\text{pH} \sim 7$, the hydrolysis process to release MB molecules is negligible.

Table 1. Effect of pH on removal of MB after 30 minutes of Cu-BTC in adsorption processes.

pH	C_t (mg/L)	H (%)	q_t (mg/g)
2.98	9.49	5.1	0.9
5.00	6.92	30.9	5.6
7.24	7.24	32.0	5.8
9.01	6.80	27.4	5.0
10.85	4.43	28.3	5.1

Note: Experimental conditions include 25°C , 0.011 g Cu-BTC, and 20 mL of 10 mg/L MB solution.

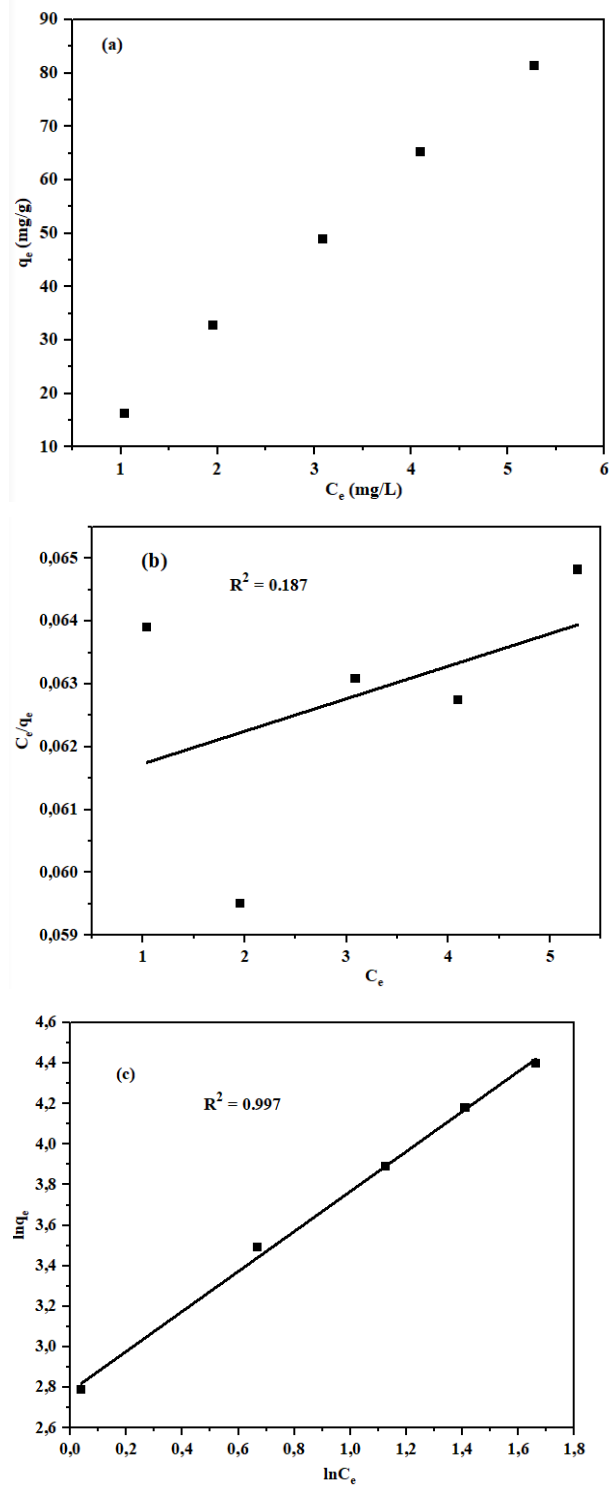
3.3. Isothermal and Kinetics of MB adsorption

The ability and mechanism of MB dye adsorption of Cu-BTC were investigated and predicted through adsorption experiments. The isotherm of the adsorption process explains the reaction mechanism between MB molecules and Cu-BTC, helping to optimize the factors affecting the adsorption process. Kinetic models were studied to better explain the reaction mechanism by analyzing adsorption capacity over time.

Figure 6 shows the isotherm modeling results of MB onto Cu-BTC, and the model parameters of the three isotherms are summarized in Table 2. The Freundlich isotherm model fits the concentration quite well. Test (correlation coefficient $R^2 = 0.9968$). The Temkin model ($R^2 = 0.9503$) fits reasonably well. The value $n = 1.01$ for the Freundlich isotherm model demonstrates the suitability of this model with experimental data. The results show the adsorption mechanism on heterogeneous surfaces, heterogeneous surfaces, and multilayer adsorption, which is also consistent with the characteristics of the synthesized materials. However, the maximum adsorption capacity of the material calculated according to the Langmuir model reached 1,929.5 mg/g, higher than the absorption capacity of other materials, such as nano Fe_3O_4 (161.8 mg/g), tannic acid/graphene nanocomposite (200 mg/g) [28]. Due to its high adsorption capacity and simple synthesis process, Cu-BTC is considered one of the essential materials for MB removal.

Table 2. Parameter values of Langmuir, Freundlich, and Temkin adsorption isotherm equations of MB on Cu-BTC.

Isotherms	Parameters	Value
Langmuir	q_m (mg/g)	1,929.5
	K_L (L/mg)	0.0085
	R^2	0.187
Freundlich	K_F [(mg/g)(L/mg) $^{1/n}$]	16.139
	n	1.01
	R^2	0.997
Temkin	K_T (L/g)	1.30
	b_T (J/mol)	63.15
	R^2	0.950



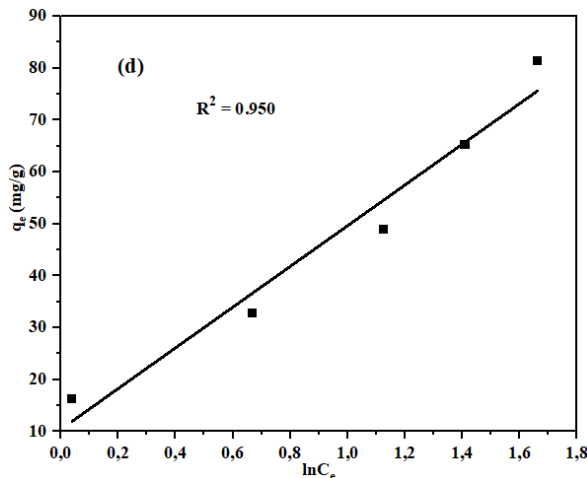


Figure 6. The adsorption isotherm of MB on Cu-BTC (a), (b) Langmuir adsorption model, (c) Freundlich adsorption model, (d) Temkin adsorption model.

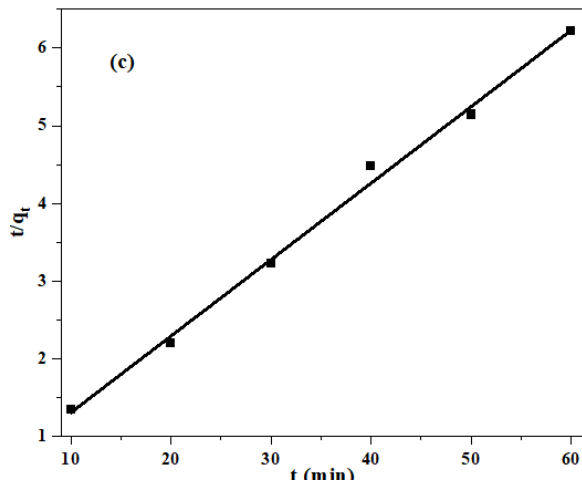
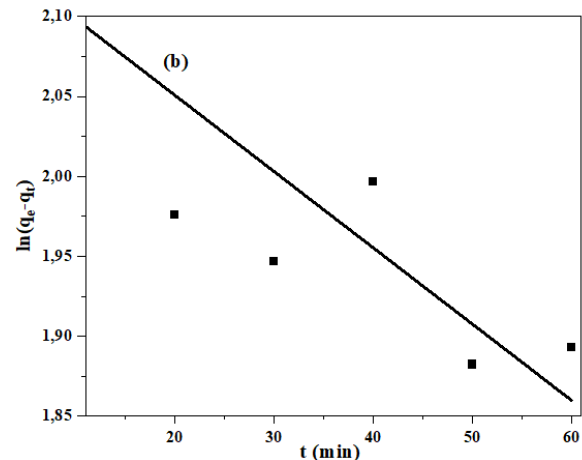
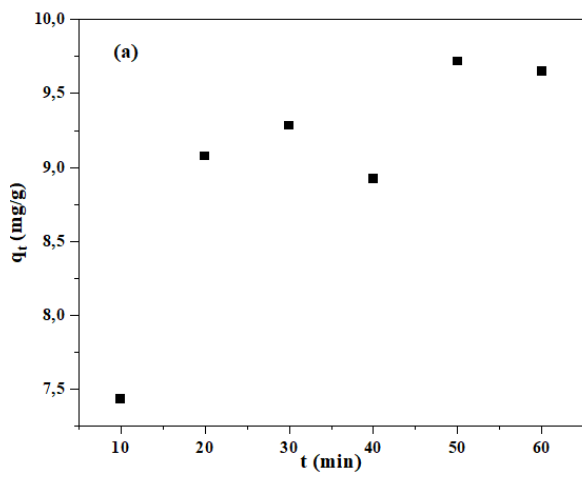
Initial concentration and adsorption time are essential parameters for the adsorption capacity of MB on Cu-BTC. As shown in Table 3, at the same initial concentration, the adsorption capacity of MB on the Cu-BTC organometallic framework material increased as the adsorption time increased. Similarly, in Figure 7a, at five different initial concentrations of MB of 10, 20, 30, 40, and 50 mg/L, the adsorption capacity of MB on the Cu-BTC organometallic framework material increased when The initial concentration of MB increased. That shows that the adsorption efficiency depends on the adsorption time and initial concentration of MB.

Table 3. Effect of time on MB adsorption of Cu-BTC in the adsorption process.

Time (min)	C _t (mg/L)	H (%)
10	5.91	40.9
20	5.01	49.9
30	4.89	51.1
40	5.09	49.1
50	4.65	53.5
60	4.69	53.1

Note: Experimental conditions are pH = 7.24; 25 °C, 0.011 g Cu-BTC; 20 mL of MB solution, initial concentration of MB is 10 mg/L.

The three models are shown in Figure 8, and their kinetic parameters are presented in Table 4.



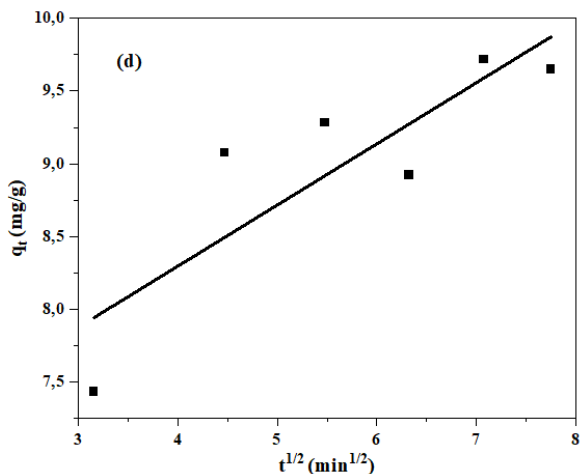


Figure 7. Effect of time on adsorption capacity (a), model of apparent first-order (b), apparent second-order (c), intra-particle diffusion (d) for MB adsorption on Cu-BTC.

Note: Experimental conditions are pH = 7.24; 25 °C, 0.011 g Cu-BTC; 20 mL of MB solution, the initial concentrations of MB are 10, 20, 30, 40, and 50 mg/L, respectively.

Table 4. Parameters of the apparent kinetic equation of MB adsorption onto Cu-BTC with an initial 10 mg/L concentration.

Kinetic model	Parameter	Value
First-order apparent model	k_1 (min ⁻¹)	-8.10 ⁻⁵
	$q_{e,cal}$ (mg/g)	8.55
	$q_{e,exp}$ (mg/g)	16.29
	R^2	0.5957
Second-order apparent model	k_2 (g/mg.min)	0.0296
	$q_{e,cal}$ (mg/g)	10.16
	$q_{e,exp}$ (mg/g)	16.29
	R^2	0.9948
Intraparticle diffusion model	k_i (mg/g.min ^{1/2})	0.42075
	C (mg/g)	6.61
	R^2	0.6692

From Table 4, it can be seen that the correlation coefficient R^2 of the apparent quadratic model ($R^2 = 0.9948$) is more significant than that of the clear first-order model ($R^2 = 0.5957$), and the model experimental diffusion pattern ($R^2 = 0.6692$). In addition, the equilibrium adsorption capacity value calculated according to the

apparent quadratic kinetic equation ($q_{e,cal}$) is much closer to the experimentally calculated adsorption capacity value ($q_{e,exp}$) than the value. The adsorption capacity value was calculated according to the apparent first-order kinetic equation. These results indicate that the apparent first-order model does not describe the adsorption process. From that, the apparent second-order kinetic model describes the MB adsorption process for the entire adsorption time. However, the apparent first- and second-order models could not determine the diffusion mechanism of MB adsorption on Cu-BTC MOFs, so the intra-particle diffusion model was used to determine the diffusion mechanism. Table 4 shows that the correlation coefficient model R^2 of the particle diffusion kinetics model ($R^2 = 0.6692$) is lower than that of the apparent quadratic model. The adsorption process is related to the diffusion of particles. Dispersed in the particles, it is not the only factor affecting adsorption. Therefore, the adsorption process occurs in an apparent second-order pattern and is controlled by other factors such as pH.

4. CONCLUSION

This study used a simple microwave method to synthesize Cu-BTC organometallic framework material to remove MB in water. The synthesized Cu-BTC MOFs have octahedral morphology. Studies on the effects of pH, concentration, and adsorption time showed that MB was removed according to the Freundlich isotherm adsorption model and the apparent second-order kinetic model. Therefore, the multilayer MB adsorption mechanism on the surface of Cu-BTC MOFs is not uniform and is influenced by electrostatic attraction. These characteristics show that Cu-BTC MOFs are ideal for further research on MB removal from wastewater and potential applications in environmental research.

REFERENCES

1. Sönmez, V.Z. and N. Sivri, *Change of Acute Toxicity of Dyestuff Wastewaters*. Polish Journal of Environmental Studies, 2020. **29**(1).
2. Oladoye, P.O., et al., *Methylene blue dye: Toxicity and potential technologies for elimination from (waste) water*. Results in Engineering, 2022: p. 100678.
3. Tomar, T., et al., *Bioremediation of synthetic dyes from wastewater by using microbial nanocomposites: An emerging field for water pollution management*. Biocatalysis and Agricultural Biotechnology, 2023: p. 102767.

4. Oladoye, P.O., et al., *Toxicity and decontamination strategies of Congo red dye*. Groundwater for Sustainable Development, 2022. **19**: p. 100844.

5. Andriamanantena, M., et al., *Alternative sources of red dyes with high stability and antimicrobial properties: towards an ecological and sustainable approach for five plant species from Madagascar*. Journal of Cleaner Production, 2021. **303**: p. 126979.

6. Khan, W.U., et al., *A critical review of hazardous waste generation from textile industries and associated ecological impacts*. Journal of the Indian Chemical Society, 2022: p. 100829.

7. Preethi, P.S., et al., *Bioprospecting of novel peroxidase from Streptomyces coelicolor strain SPR7 for carcinogenic azo dyes decolorization*. Chemosphere, 2023. **310**: p. 136836.

8. Bhat, S.A., et al., *Nanovertenergie: Bactericidal polymer nanocomposite beads for carcinogenic dye removal from aqueous solution*. Journal of Molecular Structure, 2023. **1284**: p. 135232.

9. Haque, M.M., et al., *Enhanced biofilm-mediated degradation of carcinogenic and mutagenic azo dye by novel bacteria isolated from tannery wastewater*. Journal of Environmental Chemical Engineering, 2023. **11**(5): p. 110731.

10. Samsami, S., et al., *Recent advances in the treatment of dye-containing wastewater from textile industries: Overview and perspectives*. Process safety and environmental protection, 2020. **143**: p. 138-163.

11. Selvi, S.K. and M. Eswaramurthi, *Treatment of textile dyeing wastewater using a low-cost adsorbent*. Materials Today: Proceedings, 2023.

12. Sağlam, S., F.N. Türk, and H. Arslanoğlu, *Use and applications of metal-organic frameworks (MOF) in dye adsorption*. Journal of Environmental Chemical Engineering, 2023: p. 110568.

13. Salahshoori, I., et al., *Advancements in wastewater Treatment: A computational analysis of adsorption characteristics of cationic dyes pollutants on amide Functionalized-MOF nanostructure MIL-53 (Al) surfaces*. Separation and Purification Technology, 2023. **319**: p. 124081.

14. Zhao, Y., et al., *Interface engineering of Ti-MOFs: Adsorption of anionic, cationic and neutral dyes in wastewater*. Journal of Molecular Structure, 2023. **1283**: p. 135268.

15. Vakili, A., et al., *The impact of activation temperature and time on the characteristics and performance of agricultural waste-based activated carbons for removing dye and residual COD from wastewater*. Journal of Cleaner Production, 2023. **382**: p. 134899.

16. Kumar, N., A. Pandey, and Y.C. Sharma, *A review on sustainable mesoporous activated carbon as adsorbent for efficient removal of hazardous dyes from industrial wastewater*. Journal of Water Process Engineering, 2023. **54**: p. 104054.

17. Hu, D.-D., et al., *Mussel inspired stable underwater superoleophobic cotton fabric combined with carbon nanotubes for efficient oil/water separation and dye adsorption*. Applied Surface Science, 2023. **631**: p. 157566.

18. Mahamud, M., et al., *Zeolite supported CdS/TiO₂/CeO₂ composite: Synthesis, characterization and photocatalytic activity for methylene blue dye degradation*. Materials Research Bulletin, 2023. **161**: p. 112176.

19. Lu, X.-Y., et al., *Design of Co-MOF nanosheets for efficient adsorption and photocatalytic degradation of organic dyes*. Journal of Molecular Structure, 2023. **1288**: p. 135796.

20. Mukherjee, D., B. Van der Bruggen, and B. Mandal, *Advancements in visible light responsive MOF composites for photocatalytic decontamination of textile wastewater: A review*. Chemosphere, 2022. **295**: p. 133835.

21. Singh, V., et al., *Highly functionalized photo-activated metal-organic frameworks for dye degradation: Recent advancements*. Materials Today Communications, 2022: p. 105180.

22. Shah, A.H., et al., *Porous Cu-based metal organic framework (Cu-MOF) for highly selective adsorption of organic pollutants*. Journal of Solid State Chemistry, 2023. **322**: p. 123935.

23. Yang, X., et al., *Encapsulated laccase in bimetallic Cu/Zn ZIFs as stable and reusable biocatalyst for decolorization of dye wastewater*. International Journal of Biological Macromolecules, 2023. **233**: p. 123410.

24. Shahbakhsh, M., et al., *Study of the one-step in situ growth synthesis of Cu-Pic coordination polymer and Cu-BTC MOF and their performances for detection of 4-Nitrophenol*. Microchemical Journal, 2023. **189**: p. 108557.

25. Yu, Y.-P., et al., *Facile synthesis of self-assembled three-dimensional flower-like Cu-MOF and its pyrolytic derivative Cu-N-C450 for diverse applications*. Journal of Environmental Chemical Engineering, 2023. **11**(2): p. 109400.

26. Faaizatunnisa, N., et al., *Facile green synthesis of core-shell magnetic MOF composites (Fe₃O₄@ SiO₂@ HKUST-1) for enhanced adsorption capacity of methylene blue*.

Nano-Structures & Nano-Objects, 2023. **34**: p. 100968.

27. Rabiee, N., et al., *Green metal-organic frameworks (MOFs) for biomedical applications*. Microporous and Mesoporous Materials, 2022. **335**: p. 111670.

28. Liu, Y., P. Ghimire, and M. Jaroniec, *Copper benzene-1, 3, 5-tricarboxylate (Cu-BTC) metal-organic framework (MOF) and porous carbon composites as efficient carbon dioxide adsorbents*. Journal of colloid and interface science, 2019. **535**: p. 122-132.

29. Qian, D., et al., *Synthesis of hierarchical porous carbon monoliths with incorporated metal-organic frameworks for enhancing volumetric based CO₂ capture capability*. ACS applied materials & interfaces, 2012. **4**(11): p. 6125-6132.

30. Kaur, R., et al., *Metal organic framework (MOF) porous octahedral nanocrystals of Cu-BTC: Synthesis, properties and enhanced adsorption properties*. Materials Research Bulletin, 2019. **109**: p. 124-133.

31. Hosseini, M., S. Zeinali, and M. Sheikhi, *Fabrication of capacitive sensor based on Cu-BTC (MOF-199) nanoporous film for detection of ethanol and methanol vapors*. Sensors and Actuators B: Chemical, 2016. **230**: p. 9-16.

32. Latha, G., N. Devarajan, and P. Suresh, *Framework copper catalyzed oxidative synthesis of quinazolinones: A benign approach using Cu₃(BTC) 2 MOF as an efficient and reusable catalyst*. ChemistrySelect, 2020. **5**(32): p. 10041-10047.

33. Chuah, C.Y. and T.-H. Bae, *Incorporation of Cu₃BTC₂ nanocrystals to increase the permeability of polymeric membranes in O₂/N₂ separation*. BMC Chemical Engineering, 2019. **1**(1): p. 1-9.

34. Mason, J.R., J.N. Weyrich, and H. Yang, *Mechanistic Study of Porosity Formation in Liquid-Assisted Mechanochemical Synthesis of Metal-Organic Framework Cu₃ (BTC) 2 for Adsorption-Based Applications*. Sustainability, 2022. **14**(15): p. 9150.

35. Irandoost, E., H. Farsi, and A. Farrokhi, *Effects of water content on electrochemical capacitive behavior of nanostructured Cu₃ (BTC) 2 MOF prepared in aqueous solution*. Electrochimica Acta, 2021. **368**: p. 137616.

36. LU, X.-t., et al., *Preparation of metal-organic frameworks Cu₃ (BTC) 2 with amino-functionalization for CO₂ adsorption*. Journal of Fuel Chemistry and Technology, 2019. **47**(3): p. 338-343.

37. Xiao, J., et al., *Cu₃BTC₂ MOF-impregnated Boron-doped Biochar Derived from Orange Peels for Enhanced NH₃ Capture*. Applied Surface Science, 2023: p. 157735.

38. Hameed, B. and A. Ahmad, *Batch adsorption of methylene blue from aqueous solution by garlic peel, an agricultural waste biomass*. Journal of hazardous materials, 2009. **164**(2-3): p. 870-875.

39. Ncibi, M.C., B. Mahjoub, and M. Seffen, *Kinetic and equilibrium studies of methylene blue biosorption by Posidonia oceanica (L.) fibres*. Journal of hazardous materials, 2007. **139**(2): p. 280-285.

40. Siew, W., et al., *Influence of various Cu/Fe ratios on the surface properties of green synthesized Cu-Fe-BTC and its relation to methylene blue adsorption*. Journal of hazardous materials, 2021. **416**: p. 125846.